

xray

by Ramisa Maliyat

Submission date: 05-May-2023 09:07AM (UTC+0530)

Submission ID: 1889533090

File name: Springer_Nature_LaTeX_Template_2_13.pdf (2.17M)

Word count: 10864

Character count: 58243

Investigating the Effectiveness of Interpretable Cost-Sensitive Neural Network for Pneumonia Detection Contemplating Data Imbalance

6

First Author^{1,2*}, Second Author^{2,3†} and Third Author^{1,2†}

^{1*}Department, Organization, Street, City, 100190, State, Country.

²Department, Organization, Street, City, 10587, State, Country.

³Department, Organization, Street, City, 610101, State, Country.

*Corresponding author(s). E-mail(s): iauthor@gmail.com;
Contributing authors: iiauthor@gmail.com; iiiauthor@gmail.com;

†These authors contributed equally to this work.

Abstract

Pneumonia is a bacterial or viral respiratory ailment that affects a lot of people, especially in impoverished and newly industrialized countries due to pollution, unclean living conditions, and overcrowding. Through early identification and treatment, which is sometimes hampered by a lack of adequate medical infrastructure, children's mortality rates in nations with a high prevalence of pneumonia can be greatly decreased. The objective of this research focuses on developing an automated approach for correctly identifying pneumonia from X-rays of the chest images in order to decrease the time needed for manual evaluation. In the study, two unbalanced datasets—the Corona Hack Chest X-Ray dataset and the Chest X-ray Images dataset—were selected. Using the transfer learning models ResNet50, VGG16, and Inception Net, pneumonia has been effectively identified in chest X-ray images. These models help with the classification issues related to locating irregularities connected to pneumonia and classifying those X-rays into two distinct categories based on detection outcomes. In the Chest X-Ray Images dataset, Inception-v3 achieved the highest accuracy of 97.43%, followed by VGG16 with 96.57% and ResNet50 had an accuracy of 96.40%. However, in the Corona Hack Chest X-Ray dataset, ResNet50 achieved the highest accuracy of 93.91%, followed by Inception-v3 with 91.04% and VGG16 with

2 Cost-Sensitive Neural Network for Pneumonia Detection

90.03%. Notably, these models were created to recognize and divide into two groups of anomalies in chest X-rays related to pneumonia. For imbalanced chest X-ray image datasets, a cost-sensitive neural network outperformed ResNet50, VGG16, and Inception-v3 by 1%, 2%, and 0.51%, respectively. However, the cost-sensitive neural network performed best for the Corona Hack Chest X-Ray dataset, outperforming the standard VGG16 and Inception-v3 models by 3% and 1%, respectively.

Keywords: Pneumonia, VGG16, ResNet-50, InceptionNet, deep learning, Chest X-ray Images, Explainable AI, Cost-sensitive neural network, LIME.

1 Introduction

A pulmonary infection called pneumonia can inflame the tiny air sacs in the lungs. Severe breathing difficulties and congestion, fever, chest pain, colds, or exhaustion are all signs of this illness. Pneumonia can range in severity from non-life-threatening to quite dangerous. The most vulnerable groups include newborn babies and young children, adults older than 65, those with health conditions, and those with compromised immune systems.¹ Every year, pneumonia claims the lives of more than 700,000 kids below the age of five, or over 2,000 per day, making it an infectious disease that claims the lives of most kids. Over 200,000 births are included in this. The majority of these deaths can be avoided.² Furthermore, it has been estimated that every year, pneumonia affects about 150 million individuals, mostly children under the age of 5[22]. In 2019, 740 180 children died from pneumonia, which is 14% of all pediatric fatalities. The 800,000 child fatalities attributed to pneumonia and diarrhea in 2017 are being reduced as part of the Global Action Plan.³ An early diagnosis of pneumonia can be helped by a cost-sensitive neural network, and pneumococcal immunizations can avoid over 400,000 child deaths each year.⁴ Early diagnosis of pneumonia is essential for full recovery since it enables early and effective medical intervention. The more quickly the infection is identified and diagnosed, may be treated to stop its spread and reduce its severity. By receiving the necessary oxygen therapy, antibiotics, or other supportive treatments in a timely manner, patients can reduce their symptoms, avoid complications, and hasten the healing process. Early detection also reduces the need for hospitalization, the likelihood that the condition will worsen, and the possibility that it will spread to other people. Therefore, it's necessary for a speedy recovery from pneumonia to obtain medical assistance as soon as symptoms arise. Two datasets—the CoronaHack Chest X-Ray dataset and the Chest X-ray Images dataset contributed to this study and both of which are freely available on Kaggle. Using both of these datasets, we used ResNet50, VGG16, and

¹www.mayoclinic.org/diseases-conditions/pneumonia/symptoms-causes/syc-20354204

²<https://data.unicef.org/topic/child-health/pneumonia/>

³<https://www.who.int/news-room/fact-sheets/detail/pneumonia>

⁴<https://ourworldindata.org/pneumonia>

InceptionNet as classification models.

The existing datasets for work involving pneumonia detection are imbalanced. To address the data inequivalence in the imbalanced dataset, we have suggested a strategy here. This is implemented by using the concept of a cost-sensitive neural network, where the weight is biased in the direction of the class with relatively few samples. Costs are taken into account in cost-sensitive learning,[24][25][26] refers to individuals who used cost-sensitive neural networks to complete various classification tasks. The issue of class imbalance has recently been identified as a significant challenge in data mining and machine learning. This issue occurs in many different sectors and, in some instances, has significant negative effects on the efficacy of learning techniques that depend on a uniform distribution of classes.[27].

LIME [14] is a local interpretable design explanation that explains the choice made by an instance in any black-box model by constructing an interpretable model specifically for that instance. LIME is a method that helps machine learning models become more transparent and understandable. This is essential to increasing the precision and dependability of their predictions, making them simpler to believe in and understand. In our study, the LIME has been used to explain the model's behavior. The main premise of LIME is that, in contrast to trying to represent a model worldwide, it is considerably simpler to estimate a black-box model locally (in the region where we want to explain the prediction) by a simple model.⁵

The following points serve as a summary of our work:

- For two imbalanced data sets, we proposed a strategy for identifying pneumonia according to chest X-ray images.
- For both datasets, we applied the idea of a cost-sensitive neural network and compared the results with those of more traditional transfer learning models including ResNet50, VGG16, and Inception Net.
- The pre-trained models are explained using explainable AI approaches called LIME.

Following is a summary of the remaining sections of this work:

Some of the relevant earlier works are listed in section 2 of the paper. The datasets' specifications are described in section 3. The cost-sensitive neural network, explainable AI techniques, and transfer learning models are some of the relevant background studies covered in section 4. An explanation of the suggested methodology is presented in section 5 and section 6. An explanation and discussion of the results of the experiment are provided in section 7 and section 8. The limitations and possible future works of our study are highlighted in section 9. In section 10, we finally conclude the paper.

50

⁵<https://www.oreilly.com/content/introduction-to-local-interpretable-model-agnostic-explanations-lime/>

2 Related Works

In this part, we have provided a comprehensive explanation of past studies that are related to our study. About three sections make up the overview: subsection 2.1 refers to research that concentrates on identifying pneumonia in x rays images. subsection 2.2 relates to studies that use explainable artificial intelligence. subsection 2.3 linked with works that use deep neural networks that are cost-sensitive to address the issue of imbalanced data.

2.1 Pneumonia Detection

One or both of the lungs may be affected by the dangerous disease pneumonia, which is typically carried on by bacteria, fungi, or viruses. Based on chest X-rays, we can identify this lung condition. A system that can evaluate medical images, such as X-rays or CT scans, and properly identify areas of the chest that may have pneumonia requires the development of algorithms that can distinguish features and patterns that are typical of pneumonia in chest imaging. The algorithm can be developed to identify these patterns and properties using a significant number of medical images that have been evaluated. Once it has been trained, the system can assess fresh medical images and instantly spot potential pneumonia indications in the chest. Enabling earlier identification and treatment of pneumonia may help doctors identify patients more accurately and rapidly, thereby improving patient outcomes. To ensure the system's accuracy and reliability, it is important to make sure it has gone through comprehensive testing and validation. It is also necessary to make sure the right safety measures are in place to prevent inaccurate diagnoses.

Based on the requirement to create systems that evaluate medical images and accurately identify regions of the the chest that may have pneumonia, we broadly categorized these works into two categories: (a) Systems built on large pre-trained architectures, such as Resnet-50, VGG16, and Inception Net, are examined. and (b) Deep learning-based techniques for identifying pneumonia in chest X-ray images

2.1.1 Transfer learning and Deep learning models

Recently, researchers looking into medical image categorization have become interested in the analysis of deep learning-based systems for detecting lung infections. Chest X-ray image quality issues, including inadequate contrast, numerous layers of objects, and blurred borders, greatly influence how accurately pneumonia can be detected in these images. From a medical as well as a practical standpoint, it is important to develop an autonomous model for figuring out pneumonia from a substantial number of images obtained from X-rays of the chest.

In order to classify both normal and abnormal chest X-rays, Tilve et al. [9] looked into the effectiveness of CNN models that had been previously trained and applied as feature extraction. They have used ResNet50, a densely connected convolutional neural network (DenseNet-121 and DeneNet-169) with

the SVM classifier. Four different CNN models were used by Elshennawy et al. [10] to illustrate a deep teaching strategy for classifying pneumonia. El Asnaoui, et al. [11] proposed automated methods for categorizing chest images into pneumonia and the normal class by implementing nine Deep Learning architectures, including CNN, VGG 16, VGG 19, DenseNet 201, Inception ResNet V2, Inception ResNet V3, Xception, Resnet 50, and MobileNet V2. ResNet 152 V2 and MobileNet V2 are implemented as two models that have been pre-trained in addition to CNN and LSTM-CNN. Higher classification accuracy was found for DensNet 201, Resnet 50, MobileNet V2, Inception-Resnet V2, and Inception V3. For diagnosing pneumonia from chest X-ray pictures, Wu et al.[12] have suggested a novel hybrid system called ACNNRF, which is an adaptive median filter CNN identification model constructed from Random Forest. According to experimental data, the ACNN-RF identification system can identify pneumonia with an average accuracy of up to 97%, making it more efficient than the previous traditional picture identification approach. To achieve a cross-validation accuracy of 90.16%, Chhikara et al.[13] constructed a deep CNN model that combines transfer learning.

Deep learning along with convolutional neural networks, one of the most recent methods to expedite the diagnosis of pneumonia, were reported in the research of Račić et al.[1] Using CNN, they correctly identified X-rays with pneumonia in 334 out of 381 images, and X-rays without pneumonia in 187 out of 205 photos. They have an accuracy rate of 88.90%. Scaled ResNet50 is a modified version of ResNet50 that was introduced by Hashmi et al.[2]. At a learning rate of 0.001, they obtained the best outcomes using SGD as the optimizer. Implementing SGD to act as an optimizer along with a learning rate of 0.001 allowed them to achieve their best performance. They acquired a 97.85% testing accuracy and a 0.070 testing loss. Rahman et al. [3] have presented a deep CNN-based transfer learning method for automatic pneumonia and its class recognition in this work. They have employed four different deep convolutional neural networks (CNNs) that have already been trained: Alex Net, ResNet18, DenseNet201, and Squeeze Net. For DenseNet20 training and testing, they have attained the best accuracy of 98%. using a series of images from chest X-rays for identifying pneumonia A VGG16 model architecture with fewer layers has been presented by Zhang et al. [4]. In this model, the max-pooling, drop operation, and reLU activation functions are all summarized into just six layers. With the VGG16 model, they have achieved an accuracy of 96.07%. Transfer learning was applied to images of chest X-rays by Chouhan et al. [5] to classify pneumonia. The pre-trained architectures that were used in this work include Alex Net, DenseNet121, Inception V3, Google Net, and ResNet18. Combining these 5 models, they've achieved a test accuracy of 96.39% and a sensitivity of 99.62%. To identify the presence of pneumonia, Ranjan et al.[6] have presented a complex VGG16 model. To identify the existence of pneumonia, they have created a Visual Group Geometry VGG16 model that relies on the advanced deep-learning technique.

6 Cost-Sensitive Neural Network for Pneumonia Detection

They've achieved 75.9% accuracy with the SGD optimizer, 93.7% with Adagrad Optimizer, and 98.9% with the Adam Optimizer. Salehi et al. [7] have suggested an automated CNN-based transfer learning technique implementing images from chest X-rays to identify pneumonia in children aged one to five. They deployed the VGG 19, Xception, ResNet 50, and DenseNet 121 the models that were already trained. The DenseNet 121, Xception , ResNet 50, and VGG 19 models all had the greatest classification accuracy results, coming in at 86.8%, 86.0%, 84.8%, and 83.6% respectively. A deep-learning strategy combining the CNN and VGG19 models has been presented by Dahmane et al.[8]. They implemented contrast-limited adaptive equalization of histograms and bi-histogram equalization as image processing techniques. They achieved 96.93% accuracy for the VGG19 model, 95.73% accuracy for the CNN model, and 99.89% accuracy when the two models were combined.

2.2 Cost Sensitive Deep Neural Network

On top of the Xception, InceptionResNet V2, DenseNet 201, and NASNet Mobile models, they applied transfer learning and achieved 96.8% accuracy. A cost-sensitive large-scale learning strategy has been designed by Ravi et al.[15] to identify pediatric pneumonia according to a chest X-ray. They used layered ensemble meta-classifiers combined with transfer learning-based deep feature fusion. On top of the Xception, InceptionResNet V2, DenseNet 201, and NASNet Mobile models, they performed transfer learning with 96.8Aanantama et al.[16] have implemented a Cost Sensitive method to train convolutional neural networks for the identification of pneumonia. They have discovered that the cost-sensitive training performed 85.1% more accurately than the non-cost-sensitive strategy, which performed 76.16% accurately. This greater degree of specificity is preferable for medical purposes where false negative errors can have a more negative effect than other errors. In order to generate automatically reliable representations of features for both the majority and minority classes, Khan et al.[17] constructed a cost-sensitive deep neural network. They looked at three commonly used cost functions, Cost-Sensitive MSE Loss, Cost-Sensitive SVM Hinge Loss, and Cost-Sensitive CE Loss, and discovered that they perform very well for both the majority and minority classes in the data set. The objective of Johnson et al. [18] is to examine existing deep-learning techniques to handle class-imbalanced data. The paper presents a summary and overview of 15 papers that studied various deep-learning strategies for data imbalances with DNNs.

2.3 Explainable Artificial Intelligence

The history of explainable artificial intelligence is outlined in this review study by Xu et al.[21], starting with expert systems and traditional machine learning methods and moving on to the most recent advancements in the contemporary setting of deep learning. The important research areas and reducing methodologies used in recent years are then briefly summarized. To detect

46

pneumonia, Yang et al.[19] have presented a deep learning technique that considers image background elements. The explainability is examined using the Grad-CAM approach. This method enhances pneumonia identification accuracy, with the best accuracy of VGG16 reaching 95.6%. The Influence score is an interaction-based methodology that Lo et al.[20] developed to exclude noisy and uninformative variables from the images. This methodology produces an environment with features that are easily comprehended and interpreted and are closely related to feature predictability. They attained a 99.7% Area-Under-Curve (AUC) in a real-world application of their approach on the Pneumonia Chest X-Ray Image data set using VGG16 and fewer than 20,000 parameters. When I-score selected explainable characteristics are used, over 98% of parameters can be reduced while still producing the same or better prediction results.

3 Background Study

3.1 Residual Networks(ResNet-50)

The conventional neural network ResNet, also known as Residual Networks, addresses the vanishing gradient issue that is frequently present in very deep convolutional neural networks (CNNs). ResNet enables the outputs from older levels to be immediately added to the outputs of stacked layers by including skip connections between layers. ResNet can effectively train deep neural networks by addressing the vanishing gradient problem and increasing the flow of gradient information throughout the network. One particular variant of the ResNet model is ResNet-50, which is designed to operate with 50 neural network layers. Within ResNet-50, there are 48 Convolution layers responsible for extracting and transforming features from the input data. Additionally, there is 1 MaxPool layer that performs downsampling to capture relevant information and 1 Average Pool layer that computes the average values across feature maps. This combination of layers, consisting of Convolution, MaxPool, and Average Pool layers, contributes to the overall architecture of ResNet-50, allowing it to effectively handle complex tasks and extract high-level features from images.

3.2 Visual Geometry Group-16(VGG16)

VGG-16, or Visual Geometry Group-16, is a 16-layer convolutional neural network. Its design consists of two or three convolutional layer blocks followed by a pooling layer, two hidden layers with 4096 nodes each, and finally a final layer. The final high-density network is the output layer, which has 1000 nodes and is turned on by Softmax. The VGG-16 architecture is characterized by its deep structure, with 16 layers, and the utilization of 3x3 filters with a stride of 1 pixel, enabling better feature extraction and quicker convergence. The VGG-16 model is effective for a variety of computer vision problems since

8 Cost-Sensitive Neural Network for Pneumonia Detection

it demonstrates faster convergence due to the employment of 3x3 filters that cover the entire network with a step size of 1 pixel.

3.3 InceptionNet

An architecture called InceptionNet, sometimes known as GoogleNet, provides inception modules—sub-networks that enable rapid training computation. InceptionNet has nine horizontally arranged inception components. It has 22 layers (27, including the pooling layers). Inception's last module makes use of global average pooling. As with any extremely deep network, it is vulnerable to the vanishing gradient problem. To avoid the network "dying out" in the middle, the authors added two additional classifiers. The total loss function is obtained by summing the auxiliary loss and the real loss.

3.4 Cost-Sensitive Neural Network

It is common practice to train neural network models to use the backpropagation of error analysis. When one class is over-represented in comparison to other classes in a dataset, it is said to be imbalanced. The problem of data imbalance is generally ignored by deep learning algorithms. On balanced data sets, these algorithms are able to produce good results, but their efficiency on imbalanced data sets cannot be assured. Cost-sensitive learning techniques address the issue of data imbalance by taking into account the expense of incorrectly classifying samples. For the missclassification of the samples, it assigns various cost values. A large error weighting can be applied to instances from the minority class in an imbalanced classification problem since they are frequently of greater significance than examples from the majority class. It is known as a Weighted Neural Network or Cost-Sensitive Neural Network when a neural network training algorithm is modified in this way. Keras neural network models are trained using the fit function, which accepts the class weight argument. Because this function is used to train all forms of neural networks, including Multilayer Perceptrons, CNN, and RNN, the class weighting capability is available to all of them. Compared to the training algorithm version without any class weighting, the neural network's class-weighted version performs better. Log loss⁶ is used as the cost function to improve class imbalance. We avoid using the mean square error as the cost function since the sigmoid curve matches the prediction function better than a straight line does. As a result of squaring the sigmoid function, the cost function will have a large number of local minima, which makes it very difficult to apply gradient descent to reach the global minimum. Even so, there is only one minimum to converge because log loss is a convex function. This equation will provide equal weight to the two classes, which can cause bias in a classification problem with imbalanced data.⁶

$$\text{log loss} = 1/T \sum_{k=1}^T [-(z_k * \log(z'_k)) + (1 - z_k) * \log(1 - z'_k)]$$

⁶<https://www.analyticsvidhya.com/blog/2020/10/improve-class-imbalance-class-weights/>

Where,

T is the total number of values.

z_k is the target class's actual value.

z'_k is the target class's estimated probability

The cost penalty is obtained by applying the log loss formula. After incorporating weights into the cost function, According to the updated log loss function:

$$\text{weighted log loss} = 1/T \sum_{k=1}^T [-(w_0(z_k * \log(z'_k)) + w_1((1 - z_k) * \log(1 - z'_k)))]$$

where,

w_0 is class 0's class weight.

w_1 is class 1's class weight.

Since the majority class's cost function is given less weight, the error value is also less, necessitating less frequent updating of the model coefficients. Given a weight value that is more significant for the minority class's cost function, the model's coefficients are updated more frequently and the error computation is bigger. By doing this, we may alter the bias of the model and encourage the minority class to commit fewer mistakes as a whole.

3.5 LIME

Local Interpretable Model-agnostic Explanations (LIME), one of the most popular Explainable AI approaches, are used to explain how machine learning and deep learning models work. The method aims to draw attention to image superpixels that influence the model's evaluation in either a good or negative way. Due to LIME's model independence, it is possible to comprehend what a model performs and the features it uses to build a classifier. Through the following four processes, LIME attempts to interpret.

- **Permutation of the input data :** LIME initially creates a number of fictitious data points. LIME generates a number of examples that are similar to our input image by turning on and off a portion of the superpixels in the image.
- **Determine each artificial data point's class:** In this step, every artificial data point produced by the trained model is predicted by LIME to belong to a specific class.
- **Determine each artificial data point's weight:** This phase involves calculating the cosine distance between each affected image and the original image. The more similar an image is to the original, the more significant and weighty it becomes.
- **To explain the most significant features, fit a linear classifier:** The next step is to use the weighted artificial data points to create a linear regression model. After this, each fitted coefficient is generated.

10 *Cost-Sensitive Neural Network for Pneumonia Detection*

The features that have a significant effect on the prediction are those with higher coefficients if the coefficient is ordered.

Before producing the final prediction, the model's focus on the proper areas of the image is verified using LIME, which can be used to define the model. LIME's explanation is obtained as follows:

$$\xi(x) = \operatorname{argmin}_{w \in W} L(f, g, \pi_k) + \Omega(g) \quad [14]$$

The model g optimizes the locality-aware loss $L(f,g,\pi_k)$, which measures how precisely g approximates the model to be described by f in its locality given by π_k and keeps the stated model complexity low in the interpretation for a data point k .

Here, $w \in W$ is defined as an explanation of a model, where W is a class of potential models that may be interpretable. We need to minimize $L(f,g,\pi_k)$ while having a low enough value of $\Omega(g)$. Now,

$$L(f,g,\pi_k) = \sum_{(w,w' \in W)} \pi_k(w)(f(w)-g(w'))^2$$

such that $g(w') = \omega_g w'$. and,

$\pi_k(z) = e^{(-D(k,w)^2/\sigma^2)}$, which is an exponential function defined by distance function D with width σ .

3.6 Performance Metrics

As performance measurements, we have employed accuracy, loss, precision, recall or true positive rate, and f1 score. While fitting the models, the validation split separates the data into training and validation data for each epoch. Typically, accuracy and loss rise with the number of epochs. Val accuracy starts to decline as Val loss increases (which means the model is cramming values not learning).

Precision is the proportion of actual positive results to all positive results predicted by the model. As more false positives are predicted by the model, the precision falls.

40

Recall, which is often referred to as sensitivity or the true positive rate, is the ratio of true positives to all of the actual positive cases in the dataset. It evaluates how well the model can distinguish between positive cases among all the real positive examples in the dataset.

The harmonic mean of the two measurements is used to calculate the F1-score, a statistic that combines recall and precision.

4 Data set

We predicted pneumonia using images from chest X-rays working with two different data sets. One of these is the dataset for chest X-ray images⁷, which was provided by the Guangzhou Women and Children's Medical Center and is

64

⁷ <https://www.kaggle.com/datasets/tolgadincer/labeled-chest-xray-images>

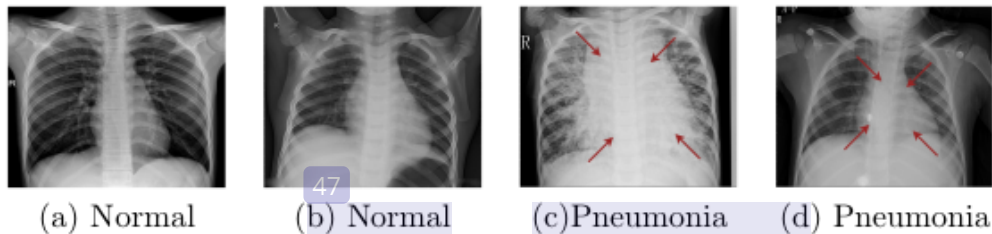


Fig. 1 Images from the Chest X-ray Images data set about normal and pneumonia-affected chest X-rays.

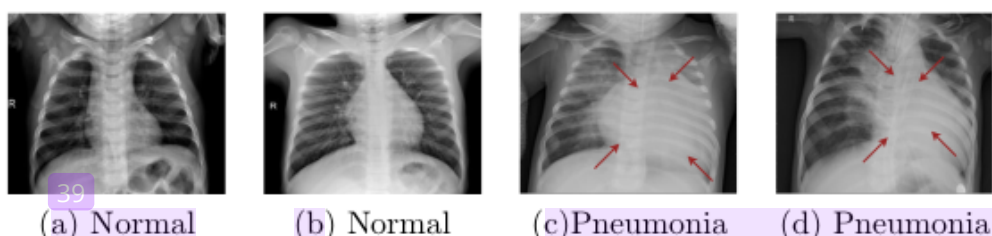


Fig. 2 Images from the CoronaHack Chest X-Ray data set about normal and pneumonia-affected chest X-rays.

accessible through Kaggle. This dataset contains 5856 JPEG images of chest X-rays. Figure 1 displays some x-ray images from normal people (a) and (b) and pneumonia patients (c) and (d).

The second dataset used in this article is CoronaHack -Chest X-Ray-Dataset⁸. 80% of the information in this dataset was gathered from various sources. Chest X-rays are taken of healthy people and those with pneumonia (Corona), as well as those who have SARS (Severe Acute Respiratory Syndrome), Streptococcus, and ARDS (Acute Respiratory Distress Syndrome). The data set consists of 5935 chest X-ray images, of which 5888 are in JPEG format. Figure 2 displays some X-ray images of normal (a) and (b) and those who have pneumonia (c) and (d).

Table 1 Data sets Details

Data set	Cases	Train	Validation	Test
15 Chest X-ray Images				
Normal	1070	221	292	
Pneumonia	3616	365	292	
CoronaHack Chest X-Ray				
Normal	1192	160	296	
Pneumonia	3538	431	296	

Three folders—train, test, and val—are used to organize both datasets. Each of these files has two sub-folders named pneumonia and normal that

⁸<https://www.kaggle.com/datasets/praveengovi/coronahack-chest-xraydataset>

contain pictures of a pneumonia-affected or normal chest x-ray. Each chest radiograph was checked for quality control before being excluded from the analysis of the chest X-ray images. The images were evaluated by two qualified doctors prior to the diagnosis being utilized to train the AI system. As a result, the images are of a high standard and are available in different sizes. Table 1 displays the distribution of the images among the folders in our data sets.

5 Methodology

This part describes the entire workflow of our research. The technique for deep learning-based pneumonia detection may be categorized into five basic sequential steps: data collection, image pre-processing, training the Models, analyzing the performances, and Explainable Artificial Intelligence. Figure 3 depicts the extensive architecture used in our methodology.

Step 1) Data collection: The first step includes choosing which images from the dataset for chest X-rays will be used for model training and evaluation.

Step 2) Image Preprocessing: The images were needed to resized since their sizes were not the same. We resized the sample images to 224*224 for every model. The datasets were then divided into the train, test, and validation sets, with ratios of 80, 10, and 10 correspondingly.

Step 3) Train the Models: As both of the datasets are imbalanced, we apply a cost-sensitive deep neural network technique where the model gives minority classes extra weight by incorporating hand-crafted weights. These techniques include the pre-trained Resnet, VGG, and InceptionNet models.

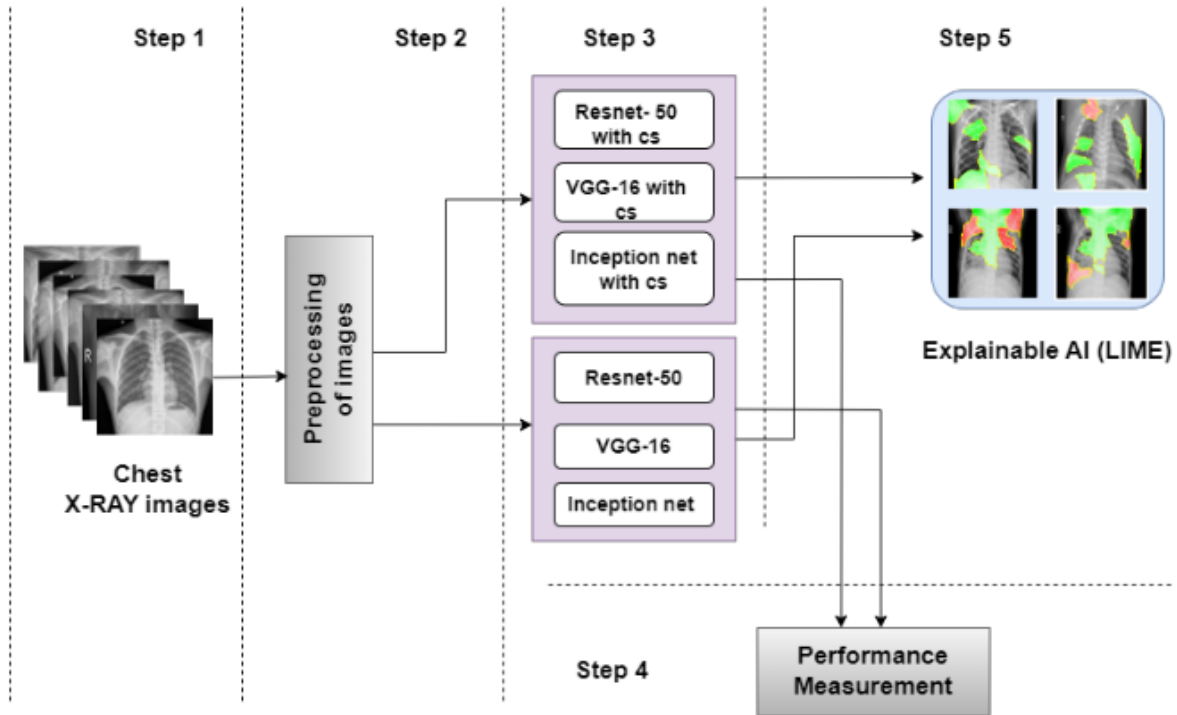
Step 4) Performance Analysis: Here, Accuracy, precision, recall, and f1-score—four distinct performance metrics, are used to evaluate each model.

Step 5) Apply Explainable Artificial Intelligence: Explainable AI approaches are used in this step to demonstrate the detection of pneumonia. All three models—including Resnet, VGG, and InceptionNet—are explained using LIME, both with and without a cost-sensitive deep neural network.

6 Model Architecture

The initial step before building a model is often preprocessing the input data. We initially bring slight changes to images to make them more suitable before training our models. In this work, we have used three transfer learning models, namely Resnet50, VGG16, and InceptionNet. The ResNet-50 model uses Max Pooling and a single Convolutional layer. The convolutional neural network-based model VGG16 was created in 2015. The VGG16 algorithm consists of an output layer, convolution, max pooling, fully connected layers, and layers with a Relu activation layer. Inception is a convolutional neural network that uses deep learning and has 48 layers; it was created by Google in 2015. Table 2 shows the architecture of our three transfer learning models.

These models use X-ray images as input, after that bias and weight were added to different regions of the image, and then classifying the images into

**Fig. 3** Workflow of the overall process

several groups. Here, we distinguish between two classes, normal and pneumonia. These models have a few layers with hidden layers, such as input and output. Pooling layers and fully connected layers may also be found in hidden layers. The pooling layer is implemented to improve visual qualities while reducing the dimensions of the input image without noticeably losing detail. By doing this, memory use and computational costs will be decreased. This approach also reduces the possibility of overfitting by reducing the number of parameters. We have used ReLU which performs well in deep neural networks primarily because of its rapid computation and lack of saturation for positive values. Throughout the model construction phase, a dropout method is also used to enhance performance and prevent overfitting in neural networks. In the dropout method, certain neurons are randomly turned off so they are not used in that iteration. Simply adding a dropout can boost accuracy in the network by 1-2.

Table 2 The architecture of our three transfer learning models is summarized here

Models	Total Parameters	Total layer	Activation functions	Last Layer
Resnet	23,587,712	50	Relu	conv5_block3_out
VGG 16	14,714,688	16	Softmax	block5_pool
InceptionNet	21,802,78	22	Softmax	mixed10

7 EXPERIMENT

7.1 Experimental Setup

Google Colaboratory⁹ and Jupiter Notebook were used to conduct the experiment. Each of the three sets—training, validation, and test—contained 80%, 10%, and 10% of the total number of images in the two data sets. We implement binary cross-entropy loss, which serves as a loss function for the binary classification model. Table 3 displays the optimizer, learning rate, batch size, and epoch for each model for the two data sets.

Table 3 Model hyperparameters

Data set	Models	Optimizer	Learning Rate	Batch Size	Epochs
Chest X-ray Images	Resnet50	Adam	$1e^{-5}$	8	29
	Resnet50 with cs				30
	VGG16				15
	VGG16 with cs				15
	Inception Net				12
CoronaHack Chest X-Ray	Inception Net with cs				25
	Resnet50	Adam	$1e^{-5}$	8	30
	Resnet50 with cs				45
	VGG16				15
	VGG16 with cs				15
Inception Net	Inception Net	Adam	$1e^{-5}$	8	12
	Inception Net with cs				12

7.2 Experimental Result

55

We analyzed the models by using the metrics -Accuracy, Precision, Recall, and F1-Score. The models' performance matrices for the two data sets are shown in Table 4. Figure 4 and Figure 5 display the accuracy and loss (train and validation) for ResNet50, VGG16, and Inception Net using both of the datasets. The Confusion Matrices are shown in Figure 6 and Figure 7 for each model in both data sets.

⁹<https://colab.research.google.com/>

Table 4 Performance matrices of models for Chest X-ray Images

Data set	Models	Accuracy	Precision	Recall	F1 score
Chest X-ray Images	Resnet50	96.40	92.80	100	96.27
	Resnet50 with cs	97.09	95.55	98.586	97.04
	VGG16	96.575	93.84	99.28	96.48
	VGG16 with cs	98.12	98.63	97.627	98.13
	Inception Net	97.43	97.60	97.27	97.44
	Inception Net with cs	97.95	97.26	98.61	97.93
CoronaHack Chest X-Ray	Resnet50	93.91	90.87	96.76	93.72
	Resnet50 with cs	93.24	89.52	96.71	92.98
	VGG16	90.03	82.43	97.21	89.21
	VGG16 with cs	93.58	90.54	96.40	93.37
	Inception Net	91.04	84.79	96.91	90.45
	Inception Net with cs	92.73	89.18	96	92.46

8 Result Analysis

In the analysis of the results, the Corona-Hack Chest X-Ray dataset and the Chest X-ray Image dataset are both used. The ResNet50 model achieved an F1 score of 96.27% and an accuracy of 96.40% in the Chest X-ray Image dataset. However, applying a cost-sensitive neural network improved the performance, resulting in an accuracy of 97.09% and an F1 score of 97.04%. Additionally, LIME was used to interpret the predictions of the model and comprehend how it focuses on different areas of the image.

Moving on to the Corona Hack Chest X-Ray dataset, the ResNet50 model achieved an accuracy of 93.24% and an F1 score of 92.98% after implementing a cost-sensitive neural network, with a validation accuracy of 86.29%. Similarly, the VGG16 model demonstrated improved accuracy, reaching 90.03% with an F1 score of 89.21% after applying a cost-sensitive neural network. The InceptionNet model achieved an accuracy of 92.73% and an F1 score of 92.46%, with a validation accuracy of 90.86% after incorporating a cost-sensitive neural network.

These findings highlight the effectiveness of cost-sensitive neural networks in enhancing the performance of different models on both datasets, while LIME was used for interpretability purposes in analyzing the models' predictions.

8.1 Performance of the Models

When the model becomes overfit or when the training accuracy reaches 99%, the process should be stopped. For evaluating the effectiveness of our model, 20% of the testing data with a balanced number of pneumonia and non-pneumonia patients were randomly chosen.

The Adam optimizer is used because it combines the advantages of adaptive

learning rates and momentum, making it effective for fine-tuning pre-trained models. A learning rate of le^{-5} is used to ensure a small and gradual update to the weights, allowing the model to learn from the new dataset without the gradual update to the pre-trained weights. As a result, overfitting is avoided, and the learning process is stable.

8.1.1 Resnet 50

ResNet is a pre-trained model, which indicates that it was developed and trained by another person to address a related issue. With regard to the chest X-ray image dataset, Due to some of the instances' classification being arbitrary, the loss curve in fig.4 (a) using resnet is fluctuating. Because the model is unable to accurately predict certain scenarios. As the model attempts to find the balance between minimizing the training loss and generalizing to the validation data, as a result, the validation loss curve may fluctuate. The accuracy of this model is not increasing as a result of loading pre-trained weight. In this model, we got an accuracy of 96.40% and 96.27% F1 score after 29 epochs with a training loss 1.02%. Since we have achieved 100% recall because the model predicts that there are no false negatives. We have reached this accuracy by tuning the hyperparameters several times. With the aid of this model, the vanishing gradient issue can be solved.

After using a cost-sensitive neural network, the Resnet50 model provided an accuracy that is 97.09% and 97.04% F1-score as shown in Table 4.

In terms of accuracy, it outperformed the regular ResNet50 by 1%. fig.4 (b) shows the loss curve's stability because of using the cost-sensitive neural network after 30 epochs. The resnet 50 model achieves a validation accuracy of 79.01%, but when a cost-sensitive network is used, the validation accuracy increases to 84.13%.

In fig. 6(a), the confusion matrix shows 271 pneumonia examples and 292 normal instances are classified accurately. On the other hand, no actual normal class images are classified as normal and 21 that belong to the pneumonia class are classified as normal. For the imbalanced nature of our dataset, we developed a cost-effective neural network with a 3.75 weighted ratio. In order to detect pneumonia in a chest image, we, therefore, applied LIME for the resnet model. By implementing a cost-sensitive neural network and operating it for 30 epochs, we were able to attain a validation accuracy of 84.13% and test accuracy of 97.09%.

Confusion matrix in fig. 6(b) shows 279 pneumonia class instances and 288 normal class instances are classified accurately from the total of 584 examples after applying a cost-sensitive neural network.

69

In the case of the Corona Hack Chest X-Ray data set, an imbalanced data set may make it difficult for the model to learn from examples from the minority class, which may result in poor generalization of the validation data. As a result, the validation loss curve fig.5 (a) may fluctuate as the model tries to find a balance between minimizing the training loss and generalizing to the

validation data. The accuracy of this model does not improve as a result of loading pre-trained weight.

After 30 iterations, this model's accuracy was 93.91%, and its F1 score was 93.72%, with a training loss of 0.86%. We repeatedly tuned the hyperparameters to get this accuracy. The Resnet50 model achieved an accuracy of 93.24% and 92.98% F1-score as demonstrated in the [Table 4](#) after applying a cost-sensitive neural network. The accuracy of resnet is slightly lower after applying a cost-sensitive neural network; this could be due to poor implementation of cost-sensitive learning or poorly tuned hyperparameters utilized during training.

After 45 epochs, the loss curve is stable because of the implementation of the cost-sensitive neural network, as shown in the [fig.5 \(b\)](#). The validation accuracy for the Resnet 50 model is 90.19%, but when a cost-sensitive network is applied, it drops to 86.29%.

The confusion matrix in [fig. 7\(a\)](#) displays 269 pneumonia examples, and 287 normal occurrences are correctly identified. On the other hand, 27 images from the pneumonia class and 9 actual images from the normal class are both categorized as normal.

We developed a cost-sensitive neural network with a weighted ratio of 2.96 to account for the unbalanced nature of our dataset. We, therefore, applied LIME to the resnet model in order to identify pneumonia in a chest image. Using a cost-sensitive neural network and running it for 45 epochs, we were able to achieve a validation accuracy of 86.29% and a test accuracy of 93.24%. According to the confusion matrix in [fig. 7\(b\)](#), a cost-sensitive neural network was applied to correctly categorize 265 pneumonia class cases and 287 normal class instances from a total of 592 samples.

8.1.2 VGG16

In terms of the Chest X-ray Images data set, the validation loss curve is fluctuating as seen in [fig.4 \(c\)](#) because of the imbalance train and validation data. Another explanation can be that updates with very small batch sizes sometimes increase global loss instead of decreasing it or removing it from local minima. Selecting a small batch size may cause the issue of over fitting the majority class worse because, in the case of an unbalanced data set, the majority class receives model updates more frequently than the minority class. As a result, if the model focuses on the majority and ignores the minority, it may perform badly for the minority and display fluctuating validation loss. We have achieved 96.57% accuracy and 96.48% F1-score after 15 epochs.

After 15 epochs, the VGG16 model achieved an accuracy that is 98.12% and 98.13% F1 score with the cost-sensitive neural network shown in [Table 4](#). It performed 2% more accurately than the normal VGG16. The green line indicates the loss of the validation set shown in [fig.4 \(d\)](#) and demonstrates that the loss curve is diverging as a result of implementing the cost-sensitive neural network. VGG 16 model has a validation accuracy of 72.62%, but when a cost-sensitive network is used, the validation accuracy rises to 87.54%.

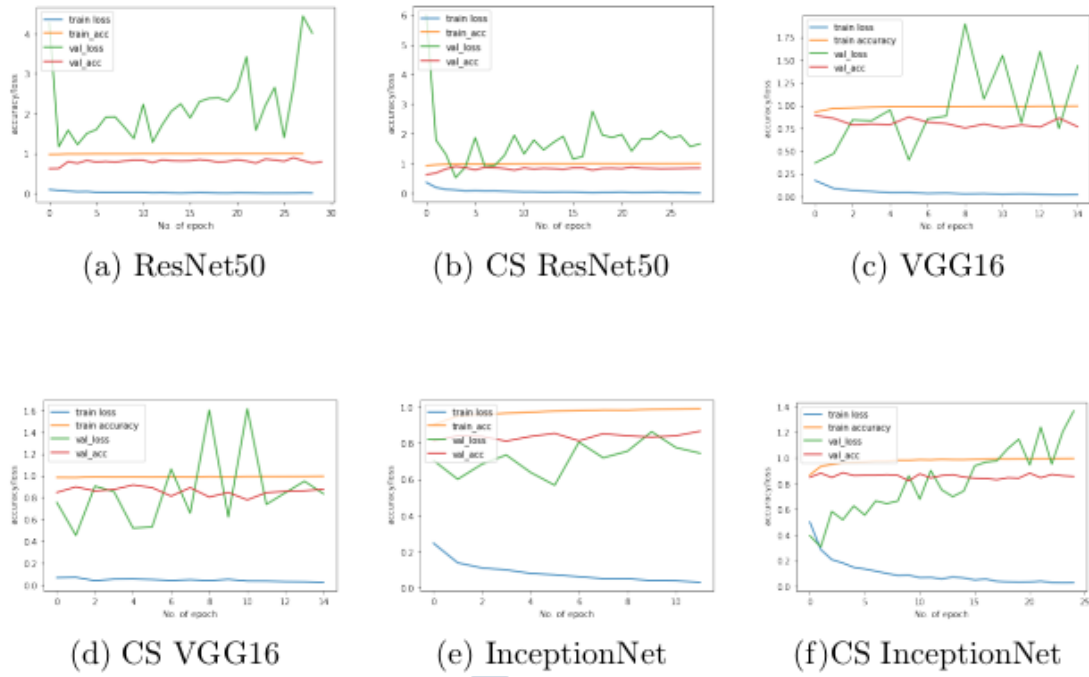


Fig. 4 Accuracy of the models during training and validation as well as their loss of the Chest X-ray Images Data set

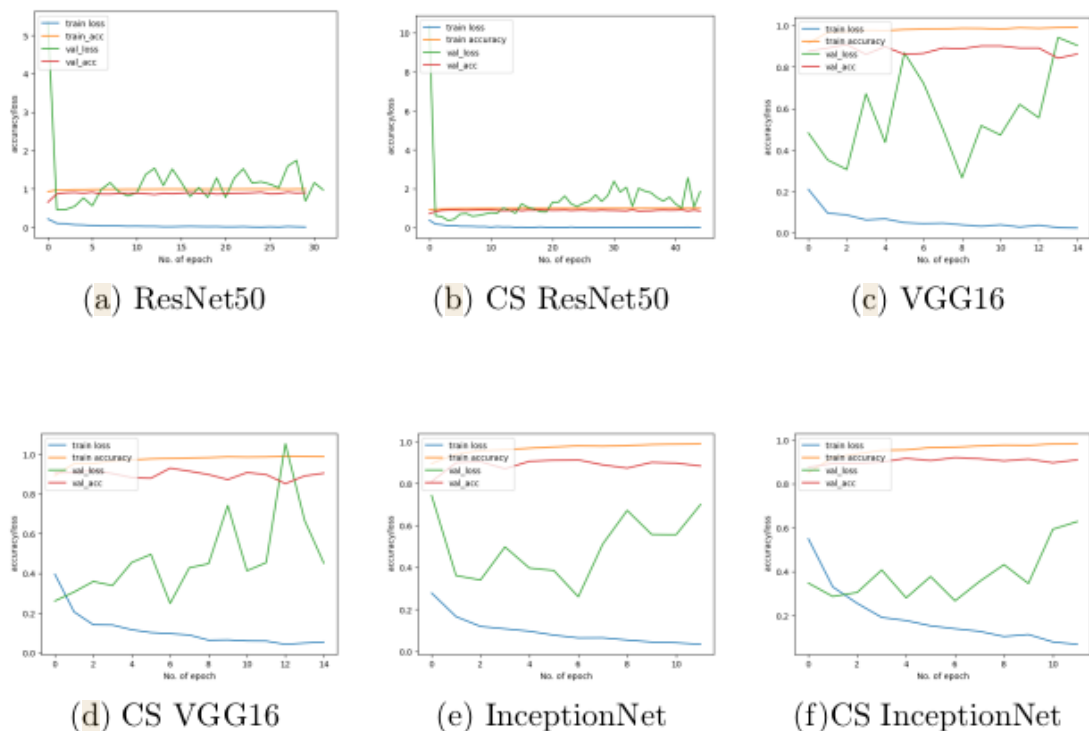


Fig. 5 Accuracy of the models during training and validation as well as their loss of the CoronaHack Chest X-Ray Data set

In fig.6 (c), the confusion matrix demonstrates that 290 normal instances and 274 pneumonia examples were correctly classified. On the other side, 18 actual pneumonia cases are classified as normal, while 2 actual normal examples are classified as pneumonia. We have developed the cost-sensitive neural network with a 3.75 weighted ratio to account for the imbalanced nature of our dataset. Therefore, we used LIME for the VGG model to identify pneumonia in a chest picture. We used a cost-effective neural network and ran it for 15 epochs, achieving a validation accuracy of 87.54% and a test accuracy of 98.12%. Confusion matrix of fig.6 (d) demonstrates that, after using a cost-sensitive neural network to classify all 584 samples, 288 pneumonia examples, and 285 normal instances were correctly identified.

30

Regarding the Corona-Hack Chest X-Ray data set, due to the imbalance of train and validation data, the validation loss curve fluctuates as shown in fig.5 (c). A model may perform well with the majority class in an imbalanced data set, but badly with the minority class, causing to a fluctuating validation loss curve. After 15 epochs, we reached 90.03% accuracy and 89.21% F1-score. After 15 iterations, the cost-sensitive neural network displayed in Table 4 helped the VGG16 model reach an accuracy of 90.03% and an F1 score of 89.21%. It performed 3% more accurately than the standard VGG16. The loss curve fluctuates as a result of implementing the cost-sensitive neural network because the model may require further training to accurately identify the minority class, therefore may cause the loss curve to fluctuate. The green line represents the loss of the validation set shown in fig.5(d). The validation accuracy of the VGG 16 model is 86.29%, but when a cost-sensitive network is utilized, it increases to 90.36%.

This confusion matrix in fig.7(c) shows that 289 instances of normal and 244 instances of pneumonia were accurately identified. On the other hand, 7 actual normal examples are labeled as pneumonia, whereas 52 actual pneumonia cases are classed as normal. To accommodate our dataset's imbalance, we created a cost-sensitive neural network with a 2.96 weighted ratio. Therefore, to detect pneumonia in a chest image, we applied LIME for the VGG model. We implemented a cost-sensitive neural network and achieved a validation accuracy of 90.36% and a test accuracy of 93.58% after 15 iterations.

Confusion matrix of fig.7 (d) shows that 268 pneumonia examples and 286 normal instances were accurately classified after implementing a cost-sensitive neural network to identify all 592 samples.

8.1.3 InceptionNet

Considering the dataset of chest X-ray images, fig.4 (e) displays the development of this model's loss and accuracy. We can see that while Validation Loss is fluctuating, training Loss is decreasing. We have achieved 97.43% accuracy and 97.44% F1-score after 12 epochs. The validation loss curve may fluctuate as a result of the imbalanced data set used to train the Inception model, which contains much more occurrences of one class than the other. This is

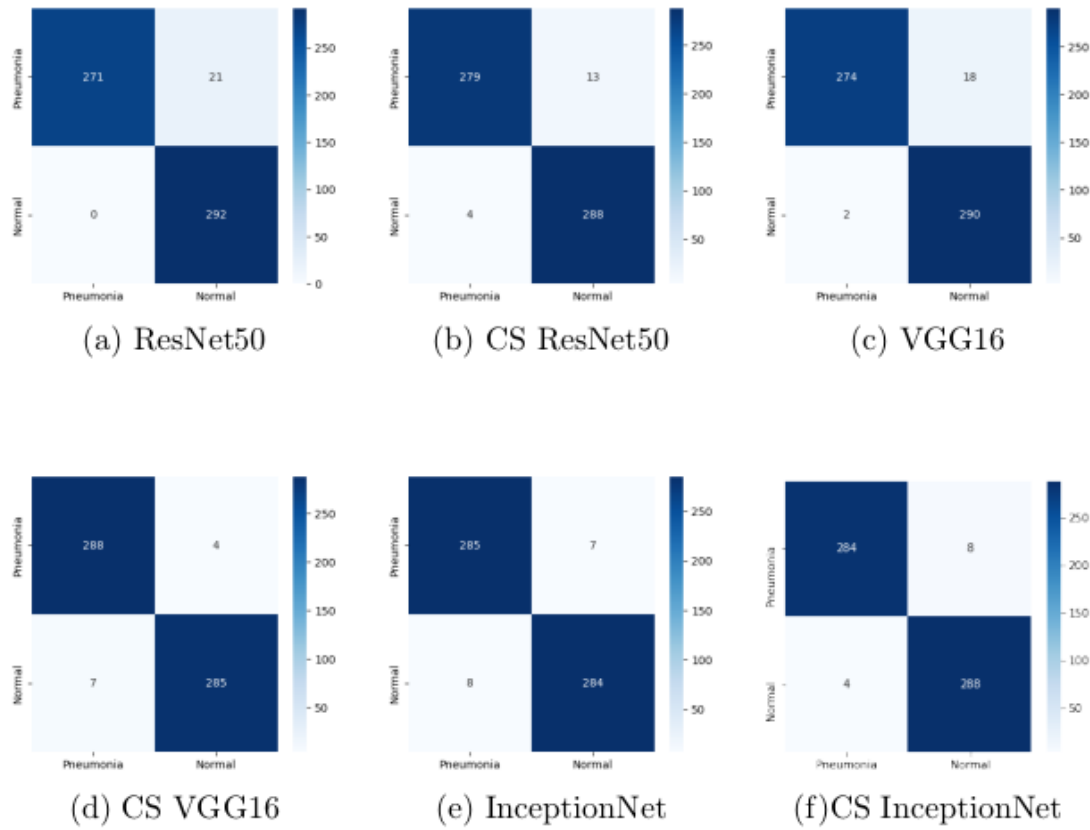


Fig. 6 Confusion matrices of all the models of Chest X-ray Images data set

due to the possibility that the model has a bias toward the majority group and may not apply properly to the minority class.

[fig.4 \(f\)](#) demonstrates that the validation accuracy is stable after applying the cost-sensitive neural network, but validation loss increases. Since the training loss is decreasing while the validation loss begins to rise after a few epochs, we can conclude that the training data are being overfitted. However, accuracy during training and validation both continued to improve because of the balance test dataset. We have 97.95% achieved accuracy and 97.93% f1-score after 25 epochs as shown in [Table 4](#). It performed 0.51% better than the standard Inception Net in terms of accuracy. The Inception Net model achieves 85.49% validation accuracy, however, when the cost-sensitive network is used, the validation accuracy improves to 86.52%.

According to the confusion matrix of [fig.6 \(e\)](#), 284 normal class and 285 pneumonia class were accurately identified, on the other hand, 8 actual positive examples are labeled as negative, while 7 actual negative situations are classified as positive for inceptionNet without cost-sensitive. To account for our dataset's imbalance, we created a cost-sensitive neural network with a 3.75 weighted ratio. Therefore, in order to detect pneumonia in a chest image, we implemented LIME for the inception net model. A cost-efficient neural network was applied, and after 25 iterations, we were able to achieve a

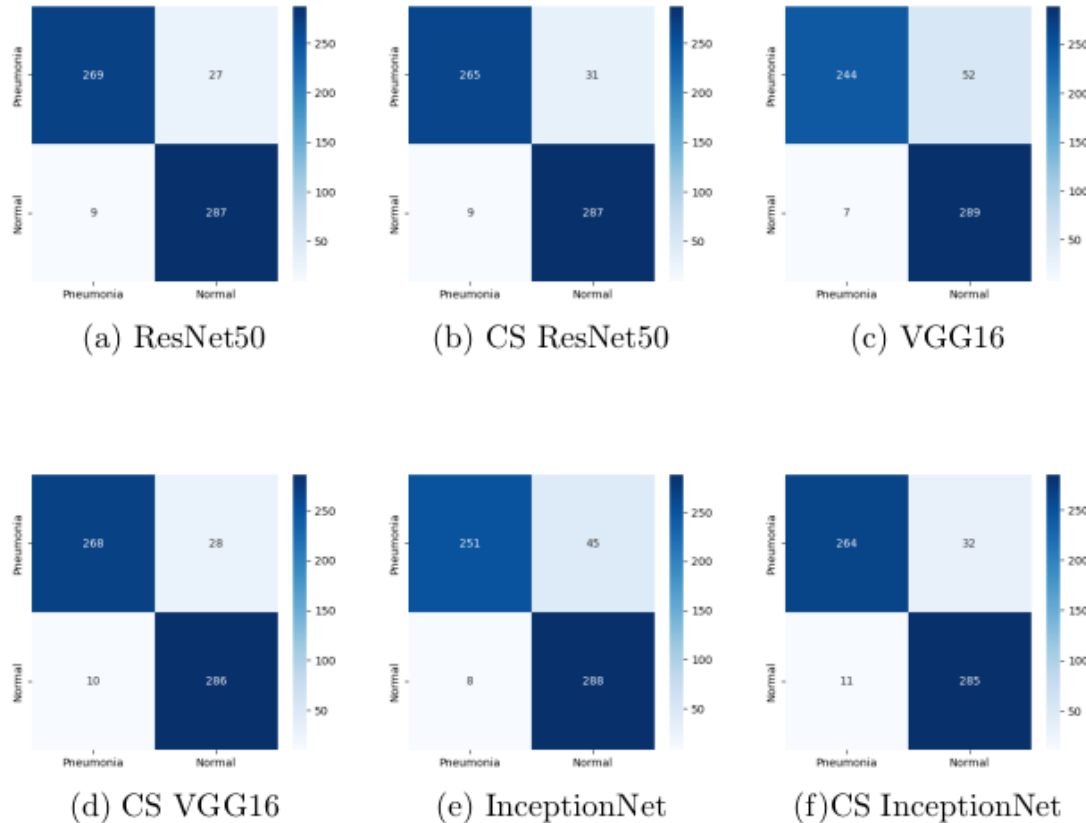


Fig. 7 Confusion matrices of all the models of Corona Hack Chest X-Ray data set

validation accuracy of 86.52% and the test accuracy of 97.95%.

Confusion matrix of [fig.6 \(f\)](#) shows that 288 normal samples and 285 pneumonia samples were accurately detected after classifying all 584 samples with a cost-sensitive neural network.

49

When it comes to the CoronaHack Chest X-Ray dataset, the development of this model's accuracy and loss is shown in [fig.5 \(e\)](#). As we can see, training loss is decreasing but validation loss fluctuates. As a result, the model may be accurate in classifying examples from the majority class with a low loss but unable to properly classify instances from the minority class, leading to a large validation loss. After 12 epochs, we achieved 91.04% accuracy and 90.45% f1-score.

The validation accuracy is consistent after using the cost-sensitive neural network, but validation loss increases, as shown by [fig.5 \(f\)](#). We may conclude that the data used for training are being overfitted because the training loss is decreasing but the validation loss starts to increase after a few epochs. But because of the balancing test dataset, accuracy during both training and validation continued to improve. After 12 epochs, we achieved 92.73% accuracy and 92.46% f1-score, as displayed in [Table 4](#). In terms of accuracy, it performed 1% better than the default Inception Net. The validation accuracy of the Inception Net model is 88.32%; however, when the cost-sensitive network

is applied, the validation accuracy increases to 90.86%.

According to the confusion matrix of fig.7 (e), 288 normal classes and 251 pneumonia classes were correctly identified; nevertheless, 8 real positive cases are labeled as negative, while 45 real negative situations are categorized as positive for inceptionNet without cost-sensitive. We developed a cost-sensitive neural network with a 2.96 weighted ratio to take into consideration the imbalance in our dataset. Therefore, we added LIME to the inception net model in order to recognize pneumonia in a chest image. We used a cost-effective neural network, and after 12 iterations, we were able to obtain a test accuracy of 92.73% and a validation accuracy of 90.86%.

Following a cost-sensitive neural network's classification of all 592 samples, the confusion matrix of fig.7(f) reveals that 285 normal examples and 264 pneumonia examples were correctly identified.

8.2 Explainable AI

All four of our transfer learning models are explained using LIME. LIME has been utilized to determine whether the chest picture has pneumonia or not. For both data sets, in each of these four scenarios, we have printed a total of eight images: true positives (1, 1), true negatives (0, 0), false positives (1, 0), and false negatives (0, 1). the region of color green increases the probability that the X-ray corresponds to the normal class. The sections that are marked with a blue line increase the probability that the X-ray corresponds to the pneumonia class. The LIME output indicates that the cost-sensitive models concentrate more on the appropriate areas of the X-ray images of the chest to make the decision.

101

For the Chest X-ray Images dataset, fig:8 (a) shows LIME output of a normal chest xray. The image is incorrectly classified by Resnet 50 and VGG 16. However, once the cost-sensitive neural network is applied, the image is accurately classified. Inception Net, however, accurately classifies the image as without cost-sensitive and with cost-sensitive.

fig:8 (b) shows that the images are correctly categorized for all models, including cost-sensitive and excluding cost-sensitive.

When a Pneumonia case is the target image, fig:8 (c) shows how explainable AI detects pneumonia. The images are appropriately categorized by Resnet50 and VGG16. However, once the cost-sensitive neural network is applied, the images are incorrectly classified. Inception Net fails to classify the image in both cases.

fig:8 (d) shows that all of the models' classifications of the images both cost-sensitive and non-cost-sensitive are correct.

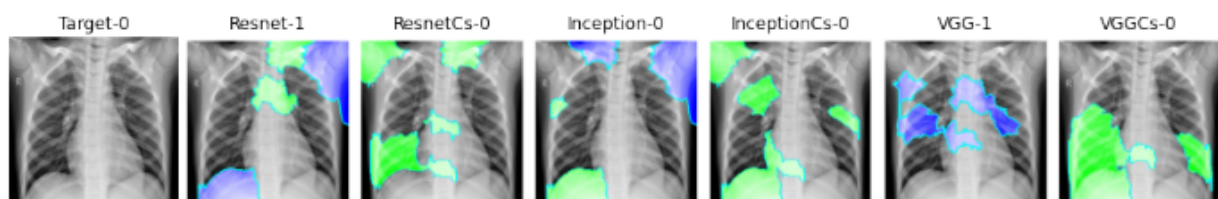
75

For the Corona Hack Chest X-Ray data set, A typical chest x-ray's LIME output is shown in fig:9 (a). All models, even those that are cost-sensitive and those that are not, have the images accurately categorized.

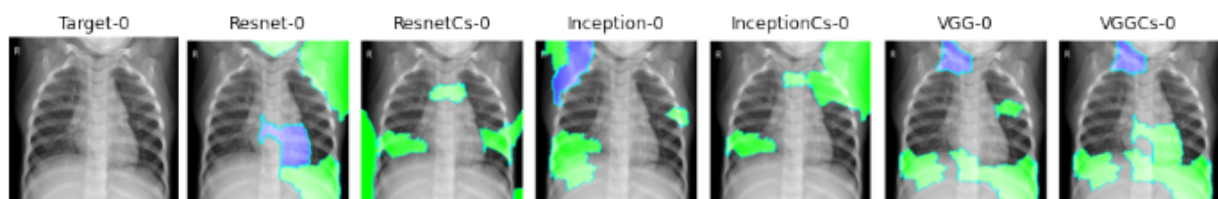
fig:9 (b) demonstrates that every model's classification of the image is inaccurate. Resnet50 and inception net, however, correctly classify the image after applying the cost-sensitive neural network. Vgg16 failed in both cases to classify the image correctly.

fig:9 (c) demonstrates how explainable AI recognizes pneumonia in the target image of a case of pneumonia. All of the models incorrectly classify the image by all of the models. However, Resnet accurately classifies the images after using the cost-sensitive neural network. Vgg16 and Inception Net both failed to classify the image in both scenarios.

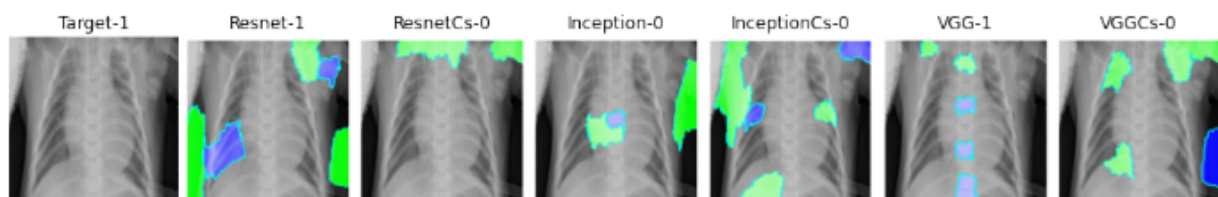
Using both cost-sensitive and non-cost-sensitive classifications of the images, fig:9 (d) illustrates that all model classifications are accurate.



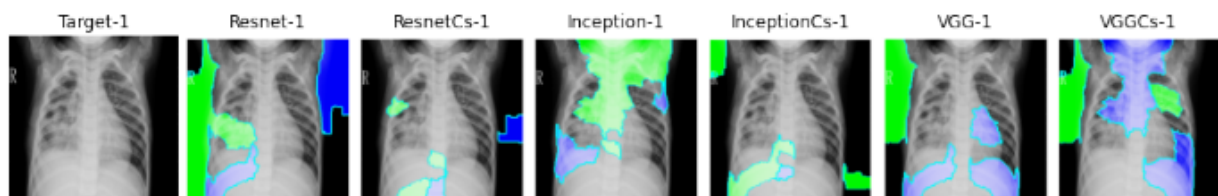
(a) An instance of the miss-classified image from the normal class



(b) An instance of correctly classified image from the normal class



(c) An instance of miss-classified image from the pneumonia class



(d) An instance of the correctly classified image from the pneumonia class

Fig. 8 Some examples of segmented LIME output (right) and the corresponding Real image (left) from the Chest X-ray Images dataset.

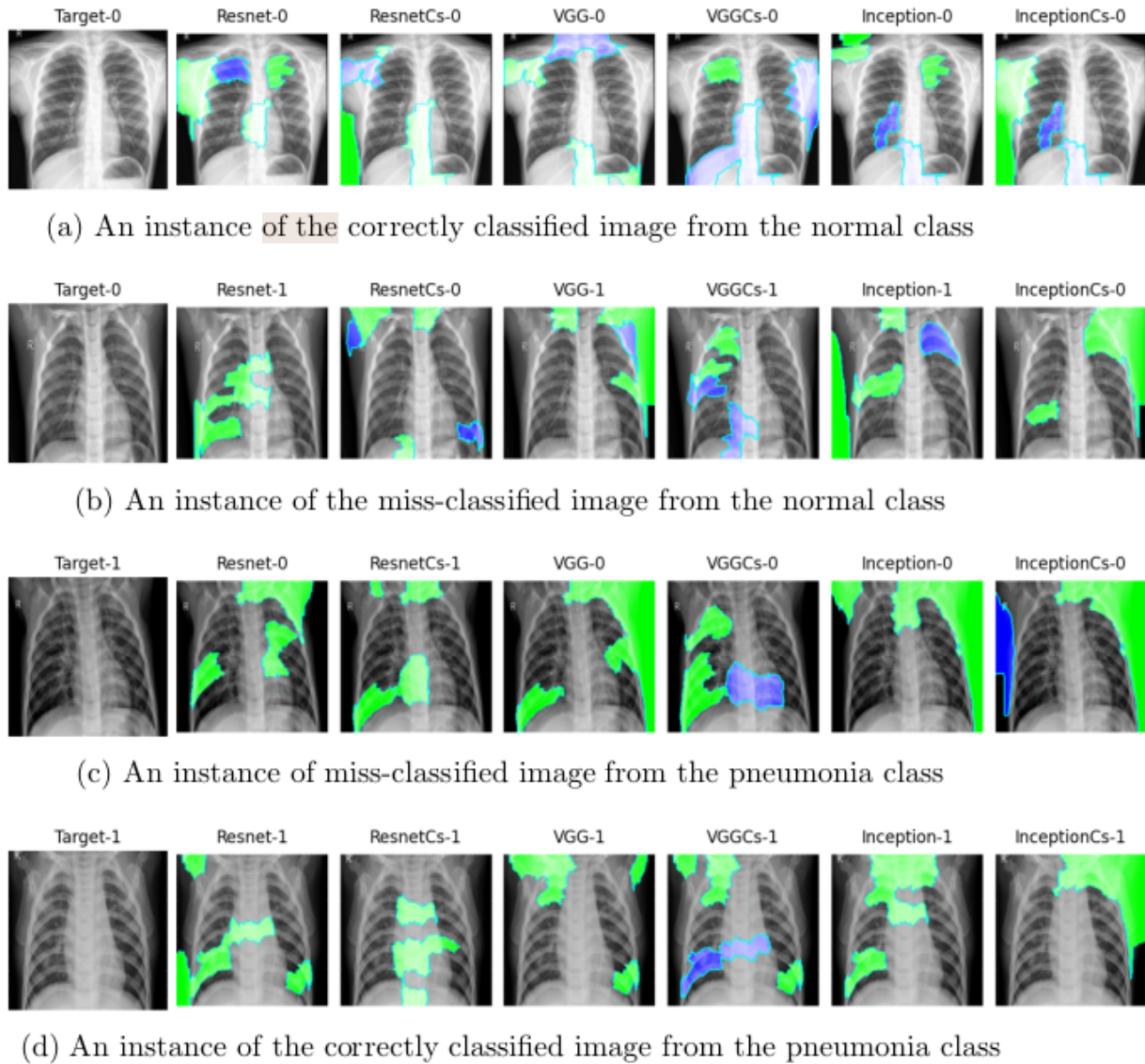


Fig. 94 Some examples of segmented LIME output (right) and the corresponding Real image (left) from the CoronaHack Chest X-Ray data set.

85 In the case of a chest X-ray image, LIME might create a neighborhood sample around a specific region of interest, and fit an interpretable model on this sample to determine the feature significance. For a proper interpretation of the image, this local background may not provide enough details because the interpretation does not include the larger context of the image, such as the overall pattern of abnormalities in the image. Since the chest x-ray images may be large or contain shadows, the models are sometimes unable to predict the correct regions, as can be seen from the LIME result.

8.3 Performance Comparison

The comparison of our three models across both datasets and cited papers is shown in [Table 5](#).

For both datasets, all three models gave better performance when we used the cost-sensitive neural network.

For the Chest X-ray Images dataset, In both cases, our VGG16 and InceptionNet outperformed the reference paper. But for Resnet-50, without using the cost-sensitive neural network, the model has an accuracy of less than 1.45 of the reference paper. After using the cost-sensitive neural network, we have achieved virtually as much accuracy as the reference paper.

All three models provided higher performances in both scenarios and outperformed the reference paper for the Corona Hack Chest X-Ray dataset.

Table 5 Comparison between the accuracy of our models to the cited paper.

Data set	Models	Reference Papers	Without cs	With cs
Chest X-ray Images	Resnet50	97.85[2]	96.40	97.09
	VGG16	93.07[3]	96.575	98.12
	InceptionNet	93.59[24]	97.43	97.95
CoronaHack Chest X-Ray	Resnet-50	92.63[32]	93.91	93.24
	VGG16	89.58[31]	90.03	93.58
	InceptionNet	90.00[29]	91.04	92.73

9 Limitations And Future Work

This work's limitations include the absence of multi-classification concerns and the sparse usage of hyperparameters. Additionally, as we have used the Explainable AI methodology, explanations are subject to change as data and decisions do. Because results may vary from person to person, this algorithm cannot be presented in general terms.

In the future, we'll look for pneumonia detection algorithms that are more accurate and investigate transfer learning techniques like DenseNet, Xception, etc. We'll also make an effort to take model weights corresponding to various algorithms into account, which should speed up the process and improve model accuracy.

10 Conclusion

This work introduces transfer learning models like the vgg16, resnet50, and inception net. These models have been used to categorize pneumonia disease from X-ray images. Furthermore, in an imbalanced dataset, the cost-sensitive

application of these models offered greater accuracy than conventional ones. However, the use of the explainable AI technique offers a better comprehension of the fundamentals and features. Using two datasets—the CoronaHack Chest X-Ray dataset and the Chest X-ray Images dataset, both of which are freely available on Kaggle, this project is more successful at distinguishing between pneumonia and non-pneumonia cases. By identifying pneumonia at an early enough stage, individuals can help treat it. In terms of the Chest X-ray Images dataset, Inceptionnet achieves the highest testing accuracy of 97.43%. After implementing a cost-sensitive neural network, this model's highest testing accuracy is 98.11%. The results indicate that, after averaging the performance metrics of precision, recall, loss, and accuracy, the Inceptionnet model performs the best in both cs and non-cs cases. Using the CoronaHack Chest X-Ray dataset, The resnet 50 model achieves the highest testing accuracy, which is 93.91%. A cost-sensitive neural network was used to achieve the highest testing accuracy for this model, which is 93.24%. To further increase the models' accuracy and make them useful for use in real life, further research is necessary.

1 Declarations

Some journals require declarations to be submitted in a standardized format. Please check the Instructions for Authors of the journal to which you are submitting to see if you need to complete this section. If yes, your manuscript must contain the following sections under the heading 'Declarations':

- Funding
- Conflict of interest/Competing interests (check journal-specific guidelines for which heading to use)
- Ethics approval
- Consent to participate
- Consent for publication
- Availability of data and materials
- Code availability
- Authors' contributions

If any of the sections are not relevant to your manuscript, please include the heading and write 'Not applicable' for that section.

References

- [1] Račić, L., Popović, T. and Šandi, S., 2021, February. Pneumonia detection using deep learning based on convolutional neural network. In 2021 25th International Conference on Information Technology (IT) (pp. 1-4). IEEE.
- [2] Hashmi, M.F., Katiyar, S., Hashmi, A.W. and Keskar, A.G., 2021. Pneumonia detection in chest X-ray images using compound scaled deep learning model. *Automatika: časopis za automatiku, mjenje, elektroniku, računarstvo i komunikacije*, 62(3-4), pp.397-406.
- [3] Rahman, T., Chowdhury, M.E., Khandakar, A., Islam, K.R., Islam, K.F., Mahbub, Z.B., Kadir, M.A. and Kashem, S., 2020. Transfer learning with deep convolutional neural network (CNN) for pneumonia detection using chest X-ray. *Applied Sciences*, 10(9), p.3233.
- [4] Zhang, D., Ren, F., Li, Y., Na, L. and Ma, Y., 2021. Pneumonia detection from chest X-ray images based on convolutional neural network. *Electronics*, 10(13), p.1512.
- [5] Chouhan, V., Singh, S.K., Khamparia, A., Gupta, D., Tiwari, P., Moreira, C., Damaševičius, R. and De Albuquerque, V.H.C., 2020. A novel transfer learning-based approach for pneumonia detection in chest X-ray images. *Applied Sciences*, 10(2), p.559.
- [6] Ranjan, A., Kumar, C., Gupta, R.K. and Misra, R., 2021, July. Transfer Learning Based Approach for Pneumonia Detection Using Customized VGG16 Deep Learning Model. In International Conference on Internet of Things and Connected Technologies (pp. 17-28). Springer, Cham.
- [7] Salehi, M., Mohammadi, R., Ghaffari, H., Sadighi, N. and Reiazi, R., 2021. Automated detection of pneumonia cases using deep transfer learning with paediatric chest X-ray images. *The British journal of radiology*, 94(1121), p.20201263.
- [8] Dahmane, O., Khelifi, M., Beladgham, M. and Kadri, I., 2021. Pneumonia detection based on transfer learning and a combination of VGG19 and a CNN built from scratch. *Indonesian Journal of Electrical Engineering and Computer Science*, 24(3), pp.1469-1480.
- [9] Tilve, A., Nayak, S., Vernekar, S., Turi, D., Shetgaonkar, P.R. and Aswale, S., 2020, February. Pneumonia detection using deep learning approaches. In 2020 International Conference on Emerging Trends in Information Technology and Engineering (ic-ETITE) (pp. 1-8). IEEE.
- [10] Elshennawy, N.M. and Ibrahim, D.M., 2020. Deep-pneumonia framework using deep learning models based on chest X-ray images. *Diagnostics*, 10(9), p.1250.

p.649.

- [5] [11] El Asnaoui, K., Chawki, Y. and Idri, A., 2021. Automated methods for detection and classification pneumonia based on x-ray images using deep learning. In Artificial intelligence and blockchain for future cybersecurity applications (pp. 257-284). Springer, Cham.
- [24] [12] Wu, H., Xie, P., Zhang, H., Li, D. and Cheng, M., 2020. Predict pneumonia with chest X-ray images based on convolutional deep neural learning networks. *Journal of Intelligent Fuzzy Systems*, 39(3), pp.2893-2907.
- [18] [13] Chhikara, P., Singh, P., Gupta, P. and Bhatia, T., 2020. Deep convolutional neural network with transfer learning for detecting pneumonia on chest X-rays. In Advances in bioinformatics, multimedia, and electronics circuits and signals (pp. 155-168). Springer, Singapore.
- [17] [14] Ribeiro, M.T., Singh, S. and Guestrin, C., 2016, August. "Why should i trust you?" Explaining the predictions of any classifier. In Proceedings of the 22nd ACM SIGKDD international conference on knowledge discovery and data mining (pp. 1135-1144).
- [27] [15] Ravi, V., Narasimhan, H. and Pham, T.D., 2022. A cost-sensitive deep learning-based meta-classifier for pediatric pneumonia classification using chest X-rays. *Expert Systems*, p.e12966.
- [16] Anantama, R., 2022. APPLICATION OF COST-SENSITIVE CONVOLUTIONAL NEURAL NETWORK FOR PNEUMONIA DETECTION. *Jurnal Ilmiah Kursor*, 11(3), pp.101-101.
- [20] [17] Khan, S.H., Hayat, M., Bennamoun, M., Sohel, F.A. and Togneri, R., 2017. Cost-sensitive learning of deep feature representations from imbalanced data. *IEEE transactions on neural networks and learning systems*, 29(8), pp.3573-3587.
- [8] [18] Johnson, J.M. and Khoshgoftaar, T.M., 2019. Survey on deep learning with class imbalance. *Journal of Big Data*, 6(1), pp.1-54.
- [29] [19] Lo, S.H. and Yin, Y., 2021. A novel interaction-based methodology towards explainable AI with better understanding of Pneumonia Chest X-ray Images. *Discover Artificial Intelligence*, 1(1), pp.1-17.
- [7] [20] Yang, Y., Mei, G. and Piccialli, F., 2022. A Deep Learning Approach Considering Image Background for Pneumonia Identification Using Explainable AI (XAI). *IEEE/ACM Transactions on Computational Biology and Bioinformatics*.

- [21] Xu, F., Uszkoreit, H., Du, Y., Fan, W., Zhao, D. and Zhu, J., 2019, October. Explainable AI: A brief survey on history, research areas, approaches and challenges. In CCF international conference on natural language processing and Chinese computing (pp. 563-574). Springer, Cham.
- [22] Rudan, I., Tomaskovic, L., Boschi-Pinto, C. and Campbell, H., 2004. Global estimate of the incidence of clinical pneumonia among children under five years of age. Bulletin of the World Health Organization, 82(12), pp.895-903.
- [23] Kalgutkar, S., Jain, V., Nair, G., Venkatesh, K., Parab, K., Deshpande, A. and Ambawade, D., 2021, April. Pneumonia Detection from Chest X-ray using Transfer Learning. In 2021 6th International Conference for Convergence in Technology (I2CT) (pp. 1-6). IEEE.
- [24] Japkowicz, N. and Stephen, S., 2002. The class imbalance problem: A systematic study. Intelligent data analysis, 6(5), pp.429-449.
- [25] Ling, C.X. and Sheng, V.S., 2008. Cost-sensitive learning and the class imbalance problem. Encyclopedia of machine learning, 2011, pp.231-235.
- [26] Zhou, Z.H. and Liu, X.Y., 2005. Training cost-sensitive neural networks with methods addressing the class imbalance problem. IEEE Transactions on knowledge and data engineering, 18(1), pp.63-77.
- [27] Japkowicz, N., 2000, July. Learning from imbalanced data sets: a comparison of various strategies. In AAAI workshop on learning from imbalanced data sets (Vol. 68, pp. 10-15). AAAI Press Menlo Park, CA.
- [28] Jain, R., Nagrath, P., Kataria, G., Kaushik, V.S. and Hemanth, D.J., 2020. Pneumonia detection in chest X-ray images using convolutional neural networks and transfer learning. Measurement, 165, p.108046.
- [29] Elgendi, M., Nasir, M.U., Tang, Q., Fletcher, R.R., Howard, N., Menon, C., Ward, R., Parker, W. and Nicolaou, S., 2020. The performance of deep neural networks in differentiating chest X-rays of COVID-19 patients from other bacterial and viral pneumonias. Frontiers in medicine, 7, p.550.
- [30] Salehi, M., Mohammadi, R., Ghaffari, H., Sadighi, N. and Reiazi, R., 2021. Automated detection of pneumonia cases using deep transfer learning with paediatric chest X-ray images. The British journal of radiology, 94(1121), p.20201263.
- [31] Patel, M., Sojitra, A., Patel, Z. and Bohara, M., 2021. Pneumonia Detection Using Transfer Learning. International Journal of Engineering Research Technology (IJERT), 10(10), pp.252-261.

- [32] Showkat, S. and Qureshi, S., 2022. Efficacy of Transfer Learning-based ResNet models in Chest X-ray image classification for detecting COVID-19 Pneumonia. *Chemometrics and Intelligent Laboratory Systems*, 224, p.104534.
- [33] VJ, S., 2021. Deep learning algorithm for COVID-19 classification using chest X-ray images. *Computational and Mathematical Methods in Medicine*, 2021.
- [34] Hilmizen, N., Bustamam, A. and Sarwinda, D., 2020, December. The multimodal deep learning for diagnosing COVID-19 pneumonia from chest CT-scan and X-ray images. In 2020 3rd international seminar on research of information technology and intelligent systems (ISRITI) (pp. 26-31). IEEE.

PRIMARY SOURCES

1	Submitted to Universidad de Salamanca Student Paper	1 %
2	Submitted to University of Hertfordshire Student Paper	1 %
3	link.springer.com Internet Source	1 %
4	eprints.iums.ac.ir Internet Source	1 %
5	Mohit Chhabra, Rajneesh Kumar. "A Smart Healthcare System based on Concatenation of ResNet50V2 and Xception Model for Detecting Pneumonia from Medical Images", 2022 International Conference on Machine Learning, Big Data, Cloud and Parallel Computing (COM-IT-CON), 2022 Publication	1 %
6	Submitted to Indian Institute of Science, Bangalore Student Paper	1 %
7	www.mdpi.com Internet Source	<1 %
8	deepai.org Internet Source	<1 %
9	Submitted to University of Northumbria at Newcastle Student Paper	<1 %

10	Submitted to Liverpool John Moores University Student Paper	<1 %
11	www.nature.com Internet Source	<1 %
12	www.researchsquare.com Internet Source	<1 %
13	Submitted to RMIT University Student Paper	<1 %
14	Submitted to Intercollege Student Paper	<1 %
15	Subhrajit Dey, Rajdeep Bhattacharya, Samir Malakar, Seyedali Mirjalili, Ram Sarkar. "Choquet fuzzy integral-based classifier ensemble technique for COVID-19 detection", <i>Computers in Biology and Medicine</i> , 2021 Publication	<1 %
16	Submitted to Edith Cowan University Student Paper	<1 %
17	par.nsf.gov Internet Source	<1 %
18	www.sigte.tel.uva.es Internet Source	<1 %
19	Submitted to University of Suffolk Student Paper	<1 %
20	researchrepository.murdoch.edu.au Internet Source	<1 %
21	www.researchgate.net Internet Source	<1 %
22	Submitted to University College London Student Paper	<1 %
23	dspace.daffodilvarsity.edu.bd:8080	

<1 %

-
- 24 Submitted to Sri Lanka Technological Campus <1 %
Student Paper
-
- 25 thesai.org <1 %
Internet Source
-
- 26 www.analyticsvidhya.com <1 %
Internet Source
-
- 27 Submitted to Roehampton University <1 %
Student Paper
-
- 28 Submitted to University of Colorado, Denver <1 %
Student Paper
-
- 29 stat.columbia.edu <1 %
Internet Source
-
- 30 assets.researchsquare.com <1 %
Internet Source
-
- 31 "Smart Computing Techniques and Applications", Springer Science and Business Media LLC, 2021 <1 %
Publication
-
- 32 doctorpenguin.com <1 %
Internet Source
-
- 33 "Artificial Intelligence and Blockchain for Future Cybersecurity Applications", Springer Science and Business Media LLC, 2021 <1 %
Publication
-
- 34 Mahmoud Aldraimli, Daniele Soria, Diana Grishchuck, Samuel Ingram et al. "A Data Science Approach for Early-Stage Prediction of Patient's Susceptibility to Acute Side Effects of Advanced Radiotherapy", Computers in Biology and Medicine, 2021 <1 %
Publication

35	www.frontiersin.org Internet Source	<1 %
36	Submitted to University of Northampton Student Paper	<1 %
37	www.enib.fr Internet Source	<1 %
38	discover.luc.edu Internet Source	<1 %
39	export.arxiv.org Internet Source	<1 %
40	Submitted to Kwame Nkrumah University of Science and Technology Student Paper	<1 %
41	Submitted to University of Kent at Canterbury Student Paper	<1 %
42	Yang Zhang, Liru Qiu, Yongkai Zhu, Long Wen, Xiaoping Luo. "A New Childhood Pneumonia Diagnosis Method Based on Fine-Grained Convolutional Neural Network", <i>Computer Modeling in Engineering & Sciences</i> , 2022 Publication	<1 %
43	rgu-repository.worktribe.com Internet Source	<1 %
44	turcomat.org Internet Source	<1 %
45	www.jjcit.org Internet Source	<1 %
46	"Advances in Computing and Data Sciences", Springer Science and Business Media LLC, 2020 Publication	<1 %
47	Sahebgoud Hanamantry Karaddi, Lakhan Dev Sharma. "Automated multi-class	<1 %

classification of lung diseases from CXR-images using pre-trained convolutional neural networks", Expert Systems with Applications, 2022

Publication

-
- 48 adib0073.medium.com <1 %
Internet Source
- 49 Mohamed Elgendi, Muhammad Umer Nasir, Qunfeng Tang, Richard Ribon Fletcher et al. "The Performance of Deep Neural Networks in Differentiating Chest X-Rays of COVID-19 Patients From Other Bacterial and Viral Pneumonias", Frontiers in Medicine, 2020
Publication
- 50 atos.net <1 %
Internet Source
- 51 Jannie Fleur V. Oraño, Marco Eraño P. Pahamotang, Rhoderick D. Malangsa. "Using Deep Learning and Adaptive Thresholding Approach for Image-based Baybayin to Tagalog Word Transliteration", 2022 IEEE 14th International Conference on Humanoid, Nanotechnology, Information Technology, Communication and Control, Environment, and Management (HNICEM), 2022
Publication
- 52 Submitted to Rochester Institute of Technology <1 %
Student Paper
- 53 Tawsifur Rahman, Muhammad E. H. Chowdhury, Amith Khandakar, Khandaker R. Islam et al. "Transfer Learning with Deep Convolutional Neural Network (CNN) for Pneumonia Detection Using Chest X-ray", Applied Sciences, 2020 <1 %
Publication

- 54 Zhi-Hua Zhou. "Training cost-sensitive neural networks with methods addressing the class imbalance problem", IEEE Transactions on Knowledge and Data Engineering, 1/2006 <1 %
Publication
-
- 55 ris.cdu.edu.au <1 %
Internet Source
-
- 56 Huaiguang Wu, Pengjie Xie, Huiyi Zhang, Daiyi Li, Ming Cheng. "Predict pneumonia with chest X-ray images based on convolutional deep neural learning networks", Journal of Intelligent & Fuzzy Systems, 2020 <1 %
Publication
-
- 57 Shashank Shetty, Ananthanarayana V S., Ajit Mahale. "MS-CheXNet: An Explainable and Lightweight Multi-Scale Dilated Network with Depthwise Separable Convolution for Prediction of Pulmonary Abnormalities in Chest Radiographs", Mathematics, 2022 <1 %
Publication
-
- 58 Subrat Kabi, Dipti Patra, Ganapati Panda. "Detection of Pneumonia from X-ray Images using Eigen Decomposition and Machine Learning techniques", 2022 International Conference on Signal and Information Processing (IConSIP), 2022 <1 %
Publication
-
- 59 Vinayakumar Ravi, Harini Narasimhan, Tuan D. Pham. "A deep learning - based for pediatric pneumonia classification using chest X - rays ", Expert Systems, 2022 <1 %
Publication
-
- 60 www.hindawi.com <1 %
Internet Source

- 61 B. Uma Maheswari, Manish Kumar Thimmaraju, V Jeeva, Mahendra Pratap Swain, Sandeep Kumar Singh, Ashok Kumar. "Development of a Website for Malaria Detection using Deep Learning", 2022 International Conference on Edge Computing and Applications (ICECAA), 2022 Publication <1 %
- 62 Jia-Min Wu, Chih-Chun Lai, Sui-Pi Chen, Cheng-Chun Lee et al. "Classification of Catheters and Tubes on Chest Radiographs Using Light-Weight Deep Convolutional Neural Networks", Research Square Platform LLC, 2023 Publication <1 %
- 63 Onur Sevli. "A deep learning - based approach for diagnosing COVID - 19 on chest x - ray images, and a test study with clinical experts", Computational Intelligence, 2022 Publication <1 %
- 64 arxiv.org Internet Source <1 %
- 65 groups.uni-paderborn.de Internet Source <1 %
- 66 ouci.dntb.gov.ua Internet Source <1 %
- 67 www.honestdocs.id Internet Source <1 %
- 68 "Innovation in Medicine and Healthcare", Springer Science and Business Media LLC, 2022 Publication <1 %
- 69 "Third International Conference on Image Processing and Capsule Networks", Springer Science and Business Media LLC, 2022 Publication <1 %

70

Submitted to Bournemouth University

Student Paper

<1 %

71

K M Abubeker, S Baskar. "B2-Net: an artificial intelligence powered machine learning framework for the classification of pneumonia in chest x-ray images", *Machine Learning: Science and Technology*, 2023

Publication

<1 %

72

Kaixiang Yang, Zhiwen Yu, C. L. Philip Chen, Wenming Cao, Jane You, Hau-San Wong. "Incremental Weighted Ensemble Broad Learning System for Imbalanced Data", *IEEE Transactions on Knowledge and Data Engineering*, 2022

Publication

<1 %

73

Mohamed Ramzy Ibrahim, Sherin M. Youssef, Karma M. Fathalla. "Abnormality detection and intelligent severity assessment of human chest computed tomography scans using deep learning: a case study on SARS-COV-2 assessment", *Journal of Ambient Intelligence and Humanized Computing*, 2021

Publication

<1 %

74

downloads.hindawi.com

Internet Source

<1 %

75

mdpi-res.com

Internet Source

<1 %

76

publications.waset.org

Internet Source

<1 %

77

riuma.uma.es

Internet Source

<1 %

78

www.aimspress.com

Internet Source

<1 %

79

www.igi-global.com

Internet Source

<1 %

-
- 80 www.ijisae.org <1 %
Internet Source
-
- 81 www.philstat.org.ph <1 %
Internet Source
-
- 82 www.semanticscholar.org <1 %
Internet Source
-
- 83 Apeksha Koul, Rajesh K. Bawa, Yogesh Kumar. "Artificial Intelligence Techniques to Predict the Airway Disorders Illness: A Systematic Review", Archives of Computational Methods in Engineering, 2022 <1 %
Publication
-
- 84 Deepak Vishwakarma, Hritik Bhandari, Nikhil Agrawal, Kriti, Jyoti Rawat. "chapter 10 Application of Deep Learning Techniques for Pneumonia Detection Using Chest X-Ray Images", IGI Global, 2023 <1 %
Publication
-
- 85 Dulani Meedeniya, Hashara Kumarasinghe, Shammi Kolonne, Chamodi Fernando, Isabel De la Torre Díez, Gonçalo Marques. "Chest X-ray analysis empowered with deep learning: A systematic review", Applied Soft Computing, 2022 <1 %
Publication
-
- 86 Peng Cao, Bo Li, Dazhe Zhao, Osmar Zaiane. "A novel cost sensitive neural network ensemble for multiclass imbalance data learning", The 2013 International Joint Conference on Neural Networks (IJCNN), 2013 <1 %
Publication
-
- 87 Rahul Gomes, Connor Kamrowski, Jordan Langlois, Papia Rozario et al. "A <1 %

Comprehensive Review of Machine Learning Used to Combat COVID-19", Diagnostics, 2022

Publication

-
- 88 Shaw-Hwa Lo, Yiqiao Yin. "A novel interaction-based methodology towards explainable AI with better understanding of Pneumonia Chest X-ray Images", Discover Artificial Intelligence, 2021 <1 %
- Publication
-
- 89 Sobhan Sheykhanvand, Zohreh Mousavi, Sina Mojtabaei, Tohid Yousefi Rezaii, Ali Farzamnia, Saeed Meshgini, Ismail Saad. "Developing an Efficient Deep Neural Network for Automatic Detection of COVID-19 Using Chest X-ray Images", Alexandria Engineering Journal, 2021 <1 %
- Publication
-
- 90 www.ncbi.nlm.nih.gov <1 %
- Internet Source
-
- 91 "Computer Vision and Image Processing", Springer Science and Business Media LLC, 2021 <1 %
- Publication
-
- 92 "Cost-Sensitive Learning of Deep Feature Representations From Imbalanced Data", IEEE Transactions on Neural Networks and Learning Systems, 2018 <1 %
- Publication
-
- 93 "Future Data and Security Engineering", Springer Science and Business Media LLC, 2019 <1 %
- Publication
-
- 94 "Sentimental Analysis and Deep Learning", Springer Science and Business Media LLC, 2022 <1 %
- Publication
-

- 95 A. Asaithambi, V. Thamilarasi. "Classification of Lung Chest X-Ray Images Using Deep Learning with Efficient Optimizers", 2023 IEEE 13th Annual Computing and Communication Workshop and Conference (CCWC), 2023 Publication <1 %
- 96 Alhassan Mabrouk, Rebeca P. Díaz Redondo, Abdelghani Dahou, Mohamed Abd Elaziz, Mohammed Kayed. "Pneumonia Detection on Chest X-ray Images Using Ensemble of Deep Convolutional Neural Networks", Applied Sciences, 2022 Publication <1 %
- 97 Oussama Dahmane, Mustapha Khelifi, Mohammed Beladgham, Ibrahim Kadri. "Pneumonia detection based on transfer learning and a combination of VGG19 and a CNN Built from scratch", Indonesian Journal of Electrical Engineering and Computer Science, 2021 Publication <1 %
- 98 Philip Gerlee. "Weak selection and the separation of eco-evo time scales using perturbation analysis", Cold Spring Harbor Laboratory, 2021 Publication <1 %
- 99 Rumana Islam, Mohammed Tarique. "Chest X-Ray Images to Differentiate COVID-19 from Pneumonia with Artificial Intelligence Techniques", International Journal of Biomedical Imaging, 2022 Publication <1 %
- 100 SHUJING LU, LI LIU, YUE LU, PATRICK S. P. WANG. "COST-SENSITIVE NEURAL NETWORK CLASSIFIERS FOR POSTCODE RECOGNITION", Publication <1 %

International Journal of Pattern Recognition and Artificial Intelligence, 2012

Publication

101

Yashvi Chandola, Jitendra Virmani, H.S.
Bhadauria, Papendra Kumar. "Review of
related work", Elsevier BV, 2021

<1 %

Publication

Exclude quotes Off

Exclude matches Off

Exclude bibliography Off